European Polymer Journal 48 (2012) 670–676

Contents lists available at SciVerse ScienceDirect

European Polymer Journal

journal homepage: www.elsevier.com/locate/europolj

Macromolecular Nanotechnology

Influence of the morphology of barium sulfate nanofibers and nanospheres on the physical properties of polyurethane nanocomposites

I.C. Romero-Ibarra *, E. Bonilla-Blancas, A. Sánchez-Solís, O. Manero

Instituto de Investigaciones en Materiales, Universidad Nacional Autónoma de México, Ciudad Universitaria, A.P. 70-360, México D.F. 04510, Mexico

ARTICLE INFO

Article history:
Received 12 August 2011
Received in revised form 20 December 2011
Accepted 1 January 2012
Available online 10 January 2012

Keywords:
Nanocomposites
Nanoparticles
Nanofiber
Barium sulfate
Polyurethane
Radio-opacity

ABSTRACT

Barium sulfate spherical agglomerates and fibers in the nanometric size range were used to prepare polyurethane (PU) nanocomposites (with 1 wt.% concentration) via melt extrusion. A detailed analysis on the effect of the morphology of the barium sulfate phase upon the mechanical, rheological and optical properties was carried out. Results show that the inclusion of the dispersed phase (with various morphologies and sizes) in the polymer matrix does not decrease the polymer mechanical properties, as is observed when particles in the micrometric size range are included. Rheological studies show that the nanocomposite containing spherical particles presents a slightly higher shear viscosity than that of the polymer matrix, in contrast to the nano-fibers viscosity which presents lower values. This is reflected in the effect of the particle morphology on the processability of the material; in contrast, the morphology has no effect on the radio-opacity of the samples. The structure and dispersion of the particles were analyzed using scanning and transmission electron microscopy. The sample with 1 wt.% nanofibers presents better processability than the system with spherical agglomerates maintaining the X-ray opacity properties.

1. Introduction

Considerable attention has been given to polymeric nanocomposites, on the basis that relatively low particle concentrations (lower than 5 wt.%) are needed to obtain improved properties with respect to conventional systems with fillers in the micrometer size range [1,2]. Mechanical and rheological properties of the resulting nanocomposites depend strongly on the shape, size and inter-particle distance (dispersion). As is well known, for obtaining a nanocomposite, at least one dimension of the dispersed particle must be in the nanometric range.

Among the important parameters to obtain improved properties are polymer matrix–nanoparticle interactions and high surface/volume ratio (high surface energy) [3,4]. Potential industrial applications face the challenge to design nanocomposites with synergy resulting from the combination and processing of the right ingredients.

Due to their high surface energy, particles tend to agglomerate, decreasing the surface area exposed to the polymer matrix, offsetting the reinforcing effects on the polymer. The challenge to processing is to obtain a well-dispersed phase to increase the interfacial area of contact with the matrix, improving the physical, rheological and thermal properties of the system [3]. To promote interfacial adhesion, chemical functionalization of particles and polymers has been considered, which leads to particle surface, inter-phase and polymer modification [5,6]. A successful composite requires phase compatibility and appropriate particle size and uniform distribution in the matrix [7].

Biocompatible polymers are amply used in biomedical applications. Sometimes, it is required to modify polymer properties to appropriate these materials to a specific use, but they must comply with strict requirements. Polyurethanes are versatile thermoplastics with applications in

---

* Corresponding author. Tel.: +52 55 56224589; fax: +52 55 56161201.
E-mail address: issis@unam.mx (I.C. Romero-Ibarra).

0014-3057/$ - see front matter © 2012 Elsevier Ltd. All rights reserved.
doi:10.1016/j.eurpolymj.2012.01.001

coatings, foams, fibers, adhesives and as elastomers [8,9]. This is a material widely used in biomedical applications (i.e., catheters, cardiac valves, tissue replacements, and so on) due to its biocompatibility [10,11]. Composite synthesis of polyurethane (PU)/$BaSO_4$ systems has attracted considerable attention due to its biocompatibility and radio-opaque properties. Radio-opaque composites have been obtained via the conventional melt processing or compounding technology; metals such as tungsten, gold or platinum are usually used, in addition to barium or bismuth salts. However, the use of such radio-opaque fillers usually leads to deteriorating polymer properties (mechanical, rheological and thermal) [12,13].

The addition of barium sulfate particles to a polymer matrix confers opacity to ultraviolet light and X-rays. This is a chemically inert salt, bio-stable, insoluble and possesses high thermal stability and retains transparency. It is amply used in materials with radio-contrasting characteristics, as filler in thermoplastics, paint-extender in coatings and as additive in pharmaceutical products [14–17]. In addition, it does not modify the biocompatibility of the polymer matrix [13,18]. When using $BaSO_4$ particles in the micrometric range, large contents are used to attain a convenient level of radio-opacity. This is, however, detrimental to mechanical properties and processing. This is the reason why smaller sizes are sought, to maintain mechanical and rheological properties and to preserve the radio-opacity of the material.

Recently, a wide variety of additives for polyurethane nanocomposites have been reported (modified Montmorillonite clays [4,19–25], carbon nanotubes, silicon carbide, carbon black [26], metal or inorganic additives, silica [27] and titanium oxides [28], among others). Notwithstanding, comparative analyses among the different morphological features of nanoparticles (spherical and fibers) and their effect on the final nanocomposite properties in the PU/$BaSO_4$ system are still lacking. This aspect is important if potential applications in the biomedical field of these systems are sought.

In this work, the effect of various morphologies of $BaSO_4$ nanoparticles on the mechanical, rheological and radio-opacity properties of the PU matrix are analyzed. Nanospheres and nanofibers were synthesized to perform a comparative analysis on the influence of particle morphology and size on the resulting properties of nanocomposites.

2. Experimental

2.1. Materials

Polyurethane Pellethane 2363-65D, a thermoplastic polyurethane elastomer, from Dow Chemical, and the anti-foam agent A-204 from Aldrich, with a purity of 99.9%, were used as received.

The nanoparticles used in this study were spherical agglomerates and $BaSO_4$ fibers. The synthesis involves the following reactants: $BaCl_2\cdot 2H_2O$ (Baker, 99%), Na_2SO_4 (Baker, 99%), disodium ethylenediaminetetraacetic acid (EDTA) EDTA–$2Na\cdot 2H_2O$ (Baker, 99%), and sodium polyacrylate salt (Fluka, 99%) Mn = 5100 g/mol.

2.2. Preparation of nano-$BaSO_4$

The synthesis of spherical $BaSO_4$ particles was reported previously [29]. It was carried out by controlled precipitation in an aqueous medium using a stabilizing agent, the salt of the ethylenediaminetetraacetic acid (EDTA), to control the size, morphology and particle size distribution (PSD). One hundred milliliters of 0.1 M $BaCl_2$ and 100 mL of 0.1 M EDTA were prepared and mixed under stirring at ambient temperature, adjusting the pH to 4. Thereafter, a third solution of 100 mL 0.1 M Na_2SO_4 was added. The resulting precipitate was decanted, washed with distilled water and dried at 110 °C for 24 h. The product was ground for mixing with the polymer.

The synthesis of the fibers was carried out mixing 100 mL of 0.1 M $BaCl_2$ and 100 mL 0.1 M of sodium polyacrylate, adjusting the pH to 7. Thereafter, 100 mL of 0.1 M Na_2SO_4 was added under stirring at ambient temperature and left to rest for 7 days. The precipitate was decanted, washed and dried at 110 °C for 24 h. The product was ground for mixing with the polymer.

2.3. Preparation of polyurethane nanocomposites

The synthesized particles were mixed with the polymer. Preparation of PU/$BaSO_4$ nanocomposites was carried out by melt extrusion in a Haake Rheocord 90 TW 100 counter-rotating twin-screw extruder of 331 mm length. The temperature profile was 175, 180, 180 and 188 °C from the feed to the die region. The pellets were dried at 110 °C for 12 h to decrease the humidity content to less than 0.06 wt.%. Thereafter, 6 g of nanoparticles were mixed with 600 g PU pellets (1 wt.%). All samples were prepared following the same thermo-mechanical history.

Foaming usually is present during processing, maybe due to rupture by the hydrolysis of PU bonds in the presence of remaining water. This degradation produces polymer segments, terminal hydroxyl groups, amines and carbon dioxide [30,31]. To improve the products, 3 g of anti-foam agent A204 (0.5 wt.%) were added during processing.

Table 1 discloses the sample compositions, wherein, for example, sample Nano-1 is formed by PU and 1 phr (parts per hundred resin) barium sulfate spherical nano-particles. Sample Micro-1 is composed of PU and 1 phr spherical micro-particles. Finally, Fiber-1 contains 1 phr nano-fibers.

2.4. Characterization

Samples for tension tests were produced by injection molding in Mannesman Demag Ergotech 50 with a L/D of

Table 1
Polyurethane/$BaSO_4$ sample compositions.

Sample	Formulation
PU	Pristine and extruded PU
Nano-1	PU + 1 phr nano$BaSO_4$/EDTA spherical agglomerates + A204
Micro-1	PU + 1 phr micro$BaSO_4$/EDTA + A204
Fiber-1	PU + 1 phr fibers $BaSO_4$/sodium polyacrylate + A204

20. The temperature profile during processing was set at 180, 210, 210 and 220 °C. Mechanical tests were carried out in an Instron 1125 following the ASTM 638-91 norm.

The samples morphology was observed in a Leica Stereoscan 440 scanning electron microscope (SEM), previously fractured using liquid nitrogen, and vacuum-coated with a gold film using a Sputtering Jeol JFC-110 equipment. The transmission electron microscopy (TEM) images were taken in a Carl Zeiss EM910 transmission electron microscope with a voltage of 120 kV at ambient temperature. The specimens were previously fractured, cut in thin layers (~70 nm) with an ultra-microtome provided with diamond cutters, under liquid nitrogen.

Rheological properties were measured in a TA-AR 1000-N stress-controlled rheometer with parallel plates of 25 mm diameter at 210 °C.

The radiology analysis was performed in a standard clinical X-ray equipment CMR MRH-II operating at 300 mA and 40 kV with a tungsten bulb of 100 mA at 0.075 s. The specimen radio-opacity was measured with an aluminum (99.9%) step-wedge bar (with 2 mm steps), following the ASTM F640-79 norm.

3. Results and discussion

SEM results for the spherical particles are shown in Fig. 1a. Spherical agglomerates of 500 nm (secondary particles) are composed of smaller particles of 50 nm size (see inset in Fig. 1a). Previous studies revealed that the primary particles have a size of ~4 nm [29]. In Fig. 1b, long fibers are observed with diameters around 100 nm.

The resultant nanocomposites (PU/various morphologies of $BaSO_4$ particles) have thermal stability in the temperature range of the melt processing. Samples do not present losses of weight in comparison with the pristine PU (TGA and DSC not shown here). Chemical reactions or phase changes were not observed during the extrusion process. The antifoam agent does not modify the polymer processing.

3.1. Structure of nanocomposites

Dispersion of the $BaSO_4$ particles in the PU matrix was determined on the fracture area of the samples. Fig. 2 shows the distribution and dispersion of 1 wt.% spherical particles in the PU matrix. The SEM and TEM images (Fig. 2a and b, respectively) reveal uniform distribution with two effects: aggregation of particles in the SEM study,

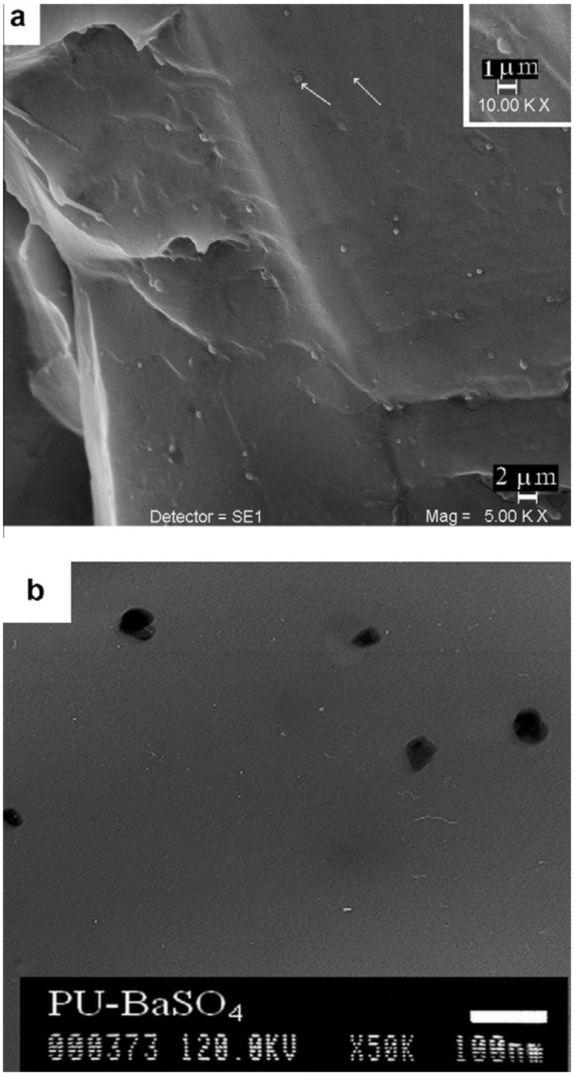

Fig. 2. (a) SEM image of a fracture of the composite. PU reinforced with spherical agglomerates of $BaSO_4$ (1 wt.%) and (b) TEM image.

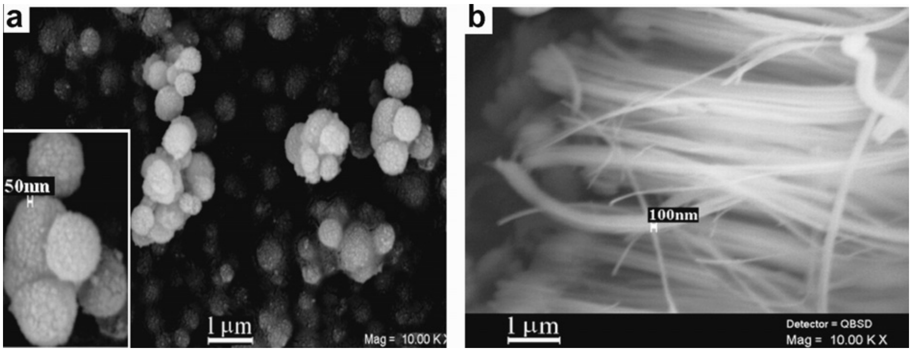

Fig. 1. SEM images: (a) spherical agglomerates of $BaSO_4$ nanoparticles and (b) $BaSO_4$ fibers.

wherein the size of the aggregates is modified with processing, increasing from 500 nm up to 1 μm (Fig. 2a); the TEM image reveals that the particle clusters are themselves formed by groups of nanoparticles of sizes around 50 nm (Fig. 2b).

These images show that the size of the agglomerates depends on the processing conditions. In neither case, big agglomerates (larger than 1 μm) or tactoids are formed, which may bring about lower mechanical properties arising from filler-type conditions instead of the reinforcement action of the smaller size particles. The agglomerates serve as stress concentration sites and fracture propagation regions, in fact limiting the expected rise in the mechanical properties. In this context, a good dispersion requires enhanced miscibility and fewer agglomerates [32–34].

Fig. 3 shows the micrograph of PU with 1 wt.% $BaSO_4$ fibers. Uniform distribution and good dispersion of particles are revealed, in the absence of tactoids. Comparing samples Nano-1 and Fiber-1 (Figs. 2a and 3a) it is evident that the fracture mechanism is different, revealing the effect of morphology on the physical properties of the nanocomposite. Alignment of polymer chains and fibers along the direction of the tension is revealed by the fracture type.

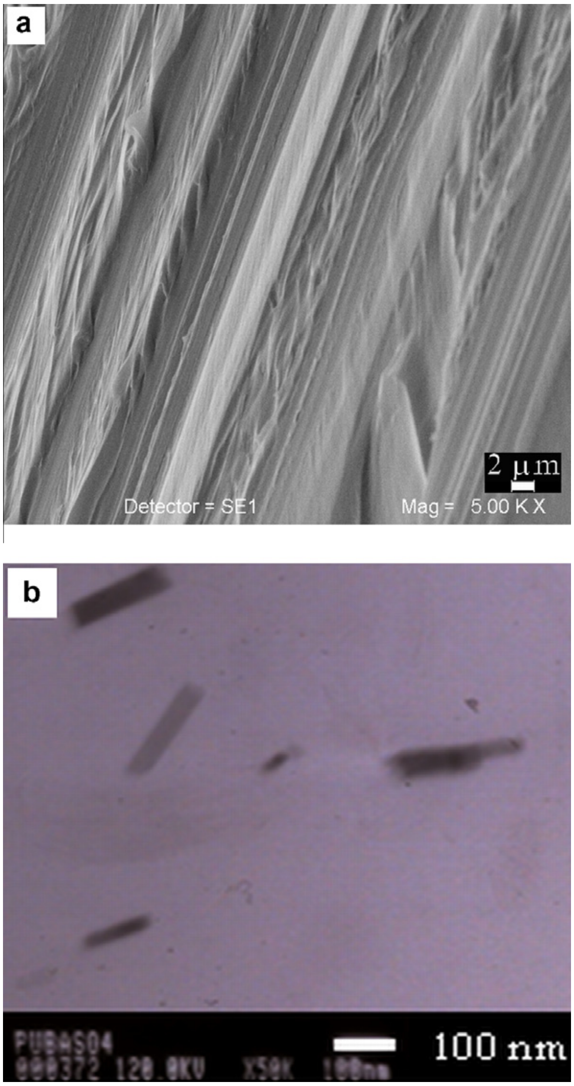

Fig. 3. (a) SEM micrograph showing an image of a fracture in the PU/fiber (1 wt.%) system and (b) TEM image.

The TEM micrograph shows the absence of agglomerates (Fig. 3b). The influence of the fibers (shown in Fig. 1b) on the morphology of the composite is shown, with some evidence of the breakage due to shear stresses during processing.

In summary, in the cases examined here a good dispersion and fine distribution of the particles are evidenced. The spherical agglomerates exhibit a particle size distribution between 50 nm and 1 μm, and the actual size depends on the processing conditions.

3.2. Mechanical properties

Table 2 displays the mechanical properties of the three systems studied here: PU with spherical morphology in the nanometric and micrometric scales and nanometric fibers. According to these results, the addition of the particles does not produce a negative effect on the mechanical properties. With respect to the matrix properties, tension strength and break of the composites remain in the same range of values. The elongation at break in all samples is larger than 560%. A slight increase of 17% in the Young modulus is measured in sample Micro-1, brought about by an increase in rigidity that is larger than in the nanometric-particle samples. In this case, the alignment of the material along the tension produces micro-crystallites. In the sample containing fibers, a decrease in the Young modulus (30%) with respect to that of the polymer is measured. This reveals that the sample Fiber-1 is more ductile or less rigid.

In summary, the addition of $BaSO_4$ nanoparticles to the PU matrix does not influence the mechanical properties negatively, as it happens when particles of larger size are mixed in higher proportions.

3.3. Rheological properties

Fig. 4 shows the shear viscosity as a function of shear rate for the systems analyzed here. At low shear rates, Newtonian behavior is apparent, followed by a shear-thinning region for moderate shear rates. The drop in viscosity is often associated to the alignment of the polymer and particles and stress-induced rupture of linkages formed by molecular interactions.

Sample Nano-1 viscosity at low shear rates is twice the value of the PU viscosity, but the largest increase is seen in

Table 2
Mechanical properties.

Sample	Tension strength (MPa)	Young's modulus (MPa)
PU	39 ± 3	252 ± 6
Nano-1	40 ± 3	248 ± 5
Micro-1	41 ± 3	295 ± 12
Fiber-1	40 ± 3	175 ± 6

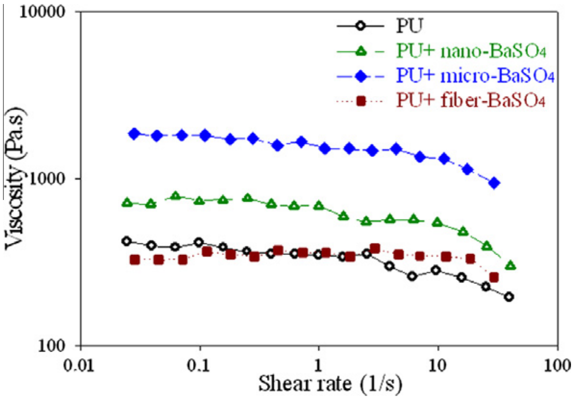

Fig. 4. Viscosity as a function of shear rate for the composites analyzed here. $BaSO_4$ particle concentration is 1 phr.

the Micro-1 sample. This behavior is characteristic of fillers, as the particles retard the motion of the composite as compared to that of the polymer. Adsorption of polymer chains onto the particles restricts the mobility of the polymer as well [34]. On the other hand, the sample containing nano-fibers exhibits the same viscosity of the polymer. This is an important qualitative change, since the particle concentration remains the same, but in contrast to the spherical particles, in this case orientation of the anisotropic particles by the shear flow seems to dominate the viscosity of the composite. It would be convenient to compare these results with those of other reports to elucidate the mechanism of nano-fiber orientation. However, a comprehensive study on the flow of these materials is still lacking, and hence the nano-fiber/polymer system deserves further understanding. In terms of processability, this system has similar characteristics of the polymer alone, which makes it a viable material and still preserves its optical properties, as discussed later.

Fig. 5 displays the storage modulus as a function of frequency. At high enough frequencies, the behavior of the composites approaches that of the polymer alone. Similar values of the plateau modulus imply similar entanglement density in the four systems. On the other end, at low frequencies, different behavior is observed. In this case, the Micro-1 sample and the sample with nano-fibers deviate from the tendency of PU. A plateau in the low frequency region is associated to polymer–particle interactions, as a solid-like behavior resulting from the formation of a tri-dimensional network is approached [35,36]. It may be feasible that the fibers and particles are interacting strongly with the matrix, which means that they are incorporated well in the polymer.

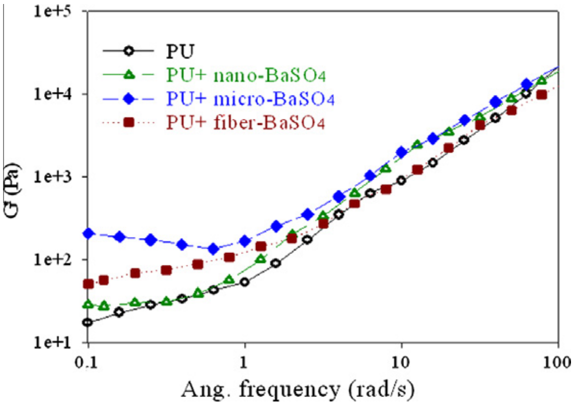

Fig. 5. Storage modulus as a function of frequency. $BaSO_4$ concentration is 1 phr.

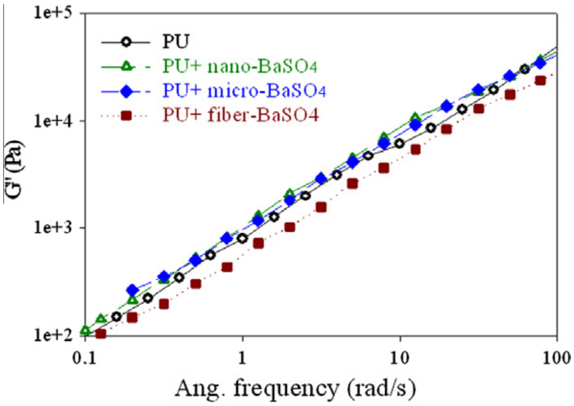

Fig. 6. Loss modulus as a function of frequency. Temperature is 190 °C.

The behavior of the loss modulus is displayed in Fig. 6. There is no deviation from the general tendency, and only a slight decrease in the modulus is observed in the composite with nano-fibers, reminiscent of the low shear viscosity shown in Fig. 4. In summary, the composite with nano-fibers displays good dispersion and adhesion to the polymer matrix, and at the same time it shows a relatively low shear viscosity that may be an advantage in terms of processability of the material.

3.4. Radio-opacity

The radio-opacity of nanocomposites is shown in Fig. 7. The absorption of X-ray radiation in each sample is uniform, reflecting the uniform dispersion of particles or fibers in the matrix. It should be mentioned that there is no qualitative difference in the radio-opacity level and they are transparent to the visible spectrum. On the contrary,

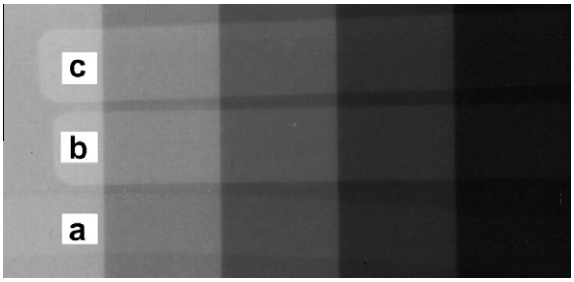

Fig. 7. Radiographs comparing: (a) PU, (b) PU + 1% $BaSO_4$ nanospheres, and (c) PU + 1% $BaSO_4$ nano-fibers.

the sample with larger size particles (Micro-1) is optically opaque.

4. Conclusions

Polyurethane/barium sulfate composites were prepared here, with the objective to relate the spherical particle or fiber morphology to the resulting mechanical, rheological and optical properties (radio-opacity) of the composite. Particles of $BaSO_4$ were synthesized via specific procedures to produce different morphologies (spherical or fibers) and different sizes (micro or nanometric). The composites were produced by melt extrusion using an anti-foam agent to prevent a decrease in the physical properties of the products.

In the past, high barium sulfate contents, sometimes more than 40 wt.%, were used to attain convenient levels of radio-opacity, with particle sizes in the micrometric range. The result of these high contents is diminishing mechanical properties, since the material becomes brittle, facing difficult processability. Here it was shown that decreasing the size of the particles or fibers, convenient levels of radio-opacity and particle or fiber dispersion were found, maintaining the mechanical, thermal and rheological properties within the level of the polyurethane properties.

A relevant result obtained was the lower viscosity of the nano-fiber composite, as compared to that of the spherical particles, with values near to those of the polyurethane matrix. The morphology of the particles does not modify the attenuation coefficient, or radio-opacity contrast. This result derives from the fact that the barium cation confers the X-ray radio-opacity and not the morphology of agglomerates. Nanoparticles of $BaSO_4$ do not diminish the transparency of the polyurethane matrix.

In summary, the nanocomposites of $PU/BaSO_4$ are good candidates for potential applications in the biomedical area, especially when non-invasive methods to detect plastic parts inside the body are sought. These nanocomposites are opaque to X-rays while maintaining a level of transparency and mechanical, thermal and rheological properties as those of the PU matrix; especially the nanofiber composite.

Acknowledgements

The authors acknowledge the technical expertise of F. Calderas in the rheological characterization, and the microscopy image work of C. Flores and O. Novelo. Also R. Cedillo for radio-opacity measurements and M. García-Sánchez for the fruitful discussions. I.C. Romero-Ibarra recognizes the financial support from CONACyT through the project 100195 and scholarship number 181930.

References

[1] Paul DR, Roberson LM. Polymer nanotechnology: nanocomposites. Polymer 2008;49(15):3187–204.

[2] Zhao J, Morgan AB, Harris JD. Rheological characterization of polystyrene–clay nanocomposites to compare the degree of exfoliation and dispersion. Polymer 2005;46(20):8641–60.

[3] Saha MC, Kabir ME, Jeelanis S. Enhancement in thermal and mechanical properties of polyurethane foam infused with nanoparticles. Mater Sci Eng A 2007;479(1–2):213–22.

[4] Lyu S, Grailer T, Belu A, Schley J, Barlett T, Hobot C, et al. Nano-adsorbent control surface properties of polyurethane. Polymer 2007;48(20):6049–55.

[5] Fernandez I, Santamaría A, Muñoz ME, Castell P. A rheological analysis of interactions in phenoxy/organoclay nanocomposites. Eur Polym J 2007;43(8):3171–6.

[6] Gurmendi U, Equiazabal JI, Nazabal J. Structure and properties of nanocomposites with a poly(trimethylene terephthalate) matrix. Eur Polym J 2008;44(6):1686–95.

[7] Olhero SM, Ferreira JM. Influence of particle size distribution an rheology and particle packing of silica-based suspensions. Powder Technol 2004;139(1):69–75.

[8] Byung Kyu K, Jang Won S, Han Mo J. Morphology and properties of waterborne polyurethane/clay nanocomposites. Eur Polym J 2003;39(1):85–91.

[9] Schön P, Bagdi K, Molnár K, Markus P, Pukánszky B, Vancso GJ. Quantitative mapping of elastic moduli at the nanoscale in phase separated polyurethanes by AFM. Eur Polym J 2011;47:692–8.

[10] Hsu S, Chou C. Enhanced biostability of polyurethane containing gold nanoparticles. Polym Degrad Stab 2004;85:675–80.

[11] Baer G, Wilson TS, Matthews DL, Maitland DJ. Shape-memory behavior of thermally stimulated polyurethane for medical applications. J Appl Polym Sci 2007;103(6):3882–92.

[12] Cabasso I, Smid J, Sahni SK. Radiopaque polymers based on acrylated phosphonate esters derived from polyols. J Appl Polym Sci 1990;41(11–12):3025–42.

[13] Guo X. Radiopaque, barium sulfate-filled biomedical compounds of a poly(ether-block-amide) copolymer. J Appl Polym Sci 2008; 109(6):4015–24.

[14] Niemann B, Veit P, Sundmacher K. Nanoparticle precipitation in reverse microemulsions: particle formation dynamics and tailoring of particle size distributions. Langmuir 2008;24(8):4320–8.

[15] Kieffer R, Mangin D, Puel F, Charcosset C. Precipitation of barium sulphate in a hollow fiber membrane contactor. Part I: investigation of particulate fouling. Chem Eng Sci 2009;64(8):1759–67.

[16] Chen Q, Shen X. Formation of mesoporous $BaSO_4$ microspheres with a larger pore size via Ostwald ripening at room temperature. Cryst Growth Des 2010;10(9):3838–42.

[17] Bala H, Fu W, Guo Y, Zhao J, Jiang Y, Ding X, et al. In situ preparation and surface modification of barium sulphate nanoparticles. Colloids Surf A 2006;274(1):71–6.

[18] Nuutinen J-P, Clerc C, Törmälä P. Mechanical properties and in vitro degradation of self-reinforced radiopaque bioresorbable polylactide fibres. J Biomater Sci Polym Ed 2003;14(7):665–76.

[19] Xu R, Manias E, Snyder AJ, Runt J. New biomedical poly(urethane urea)-layered silicate nanocomposites. Macromolecules 2001; 34(2):337–9.

[20] Finnigan B, Martin D, Halley P, Truss R, Campbell K. Morphology and properties of thermoplastic polyurethane nanocomposites incorporating hydrophilic layered silicates. Polymer 2004;45(7): 2249–60.

[21] Xiong J, Zheng Z, Jiang H, Ye S, Wang X. Reinforcement of polyurethane composites with an organically modified montmorillonite. Compos Part A Appl Sci Manuf 2007;38(1): 132–7.

[22] Jia Q, Zheng M, Chen H, Shen R. Morphologies and properties of polyurethane/epoxy resin interpenetrating network nanocomposites modified with organoclay. Mater Lett 2006;60(9–10): 1306–9.

[23] Esposito Corcione C, Prinari P, Cannoletta D, Mensitieri G, Maffezzoli A. Synthesis and characterization of clay-nanocomposite solvent-based polyurethane adhesives. Int J Adhes Adhes 2008;28(3): 91–100.

[24] Pizzato L, Lizot A, Fiorio R, Amorim C, Machado G, Giovanela M, et al. Synthesis and characterization of thermoplastic polyurethane/ nanoclay composites. Mater Sci Eng C 2008;29(2):474–8.

[25] Aurilia M, Piscitelli F, Sorrentino L, Lavorga M, Iannace S. Detailed analysis of dynamic mechanical properties of TPU nanocomposite: the role of the interfaces. Eur Polym J 2011;47(5):925–36.

[26] Gunes S, Feina C, Jana S. Evaluation of nanoparticulate fillers for development of shape memory polyurethane nanocomposites. Polymer 2008;49(9):2223–34.

[27] Bistričić L, Baranović G, Leskovac M, Govorčin Bajsić E. Hydrogen bonding and mechanical properties of thin films of polyether based polyurethane–silica nanocomposites. Eur Polym J 2010;46(10): 1975–87.

[28] Chen J, Zhou Y, Nan Q, Sun Y, Ye X, Wang Z. Synthesis, characterization and infrared emissivity study of polyurethane/TiO_2 nanocomposites. Appl Surf Sci 2007;253(23):9154–8.

[29] Romero-Ibarra IC, Rodríguez-Gattorno G, García-Sánchez MF, Sánchez-Solís A, Manero O. Hierarchically nanostructured barium sulfate fibers. Langmuir 2010;26(10):6954–9.

[30] Lu G, Kalyon DM, Yilgör I, Yilgör E. Rheology and processing of $BaSO_4$-filled medical-grade thermoplastic polyurethane. Polym Eng Sci 2004;44(10):1941–8.

[31] Hatakeyema H, Tanamachi N, Matsumura H, Hirose S, Hatakeyama T. Bio-based polyurethane composite foams with inorganic fillers studied by thermogravimetry. Thermochim Acta 2005;431(1–2): 155–60.

[32] Song M, Xia HS, Yao KJ, Hourston DJ. A study on phase morphology and surface properties of polyurethane/organoclay nanocomposite. Eur Polym J 2005;41(2):259–66.

[33] Qu M-H, Wang Y-Z, Wang C, Ge X-G, Wang D-Y, Zhou Q. A novel method for preparing poly(ethylene terephthalate)/$BaSO_4$ nanocomposites. Eur Polym J 2005;41(11):2569–74.

[34] Sánchez-Solís A, Romero-Ibarra I, Estrada M, Calderas F, Manero O. Mechanical and rheological studies on polyethylene terephthalate–montmorillonite nanocomposites. Polym Eng Sci 2004;44(6): 1094–102.

[35] Bonilla-Blancas E, Sánchez-Solís A, Manero O. Polyethylene ternary blends-clay nanocomposites. J Polym Eng 2008;28(9):553–76.

[36] Wang KH, Choi MH, Koo CM, Xu M, Chung IJ, Jang CM, et al. Morphology and physical properties of polyethylene/silicate nanocomposites prepared by melt intercalation. J Polym Sci B 2002;40(14):1454–63.